WELDING RESEARCH

SUPPLEMENT TO THE *WELDING JOURNAL*, NOVEMBER 1992

Sponsored by the American Welding Society and the Welding Research Council

Hydrogen Cracking in Duplex Stainless Steel Weld Metal

Cracking sensitivity appears related to an excess of 50% delta ferrite in the weld

BY K. SHINOZAKI, L. KE AND T. H. NORTH

ABSTRACT. Hydrogen cracking in duplex stainless steel weld metal was examined using two laboratory cracking tests (LB-TRC and WM-SERT testing). The cracking susceptibility markedly increased when the ferrite content exceeded 50% in weld metal deposited during GTA welding with Ar-10 vol-% H_2 shielding gas. Fractographic examination indicated that crack growth was inhibited by austenite plates at austenite grain boundaries. Increasing nitrogen content increased the cracking sensitivity of the ferrite phase. This detrimental effect of nitrogen was associated with increased Cr_2N precipitation in ferrite. The facets on the fracture surface of WM-SERT test specimens were parallel to the cleavage plane (100) in ferrite. The growth direction of Cr_2N precipitates in ferrite was parallel to the (100) plane, and it is suggested that the tips of these needle-like precipitates acted as sites for hydrogen crack initiation.

Introduction

Because of their desirable combination of strength and corrosion resistance, duplex stainless steels are widely used in chemical, pulp and paper, and petroleum industries. Gas tungsten arc welding using Ar-H_2 shielding gas is commonly used when joining both duplex and fully austenitic stainless steels. Hydrogen-bearing shielding gases are employed during welding since they improve weld pool fluidity, prevent surface oxidation and provide higher productivity (as a result of higher arc voltage levels during use). However, recent work has indicated that hydrogen induced cracking can occur in duplex stainless steel weld metal (Refs. 1, 2). This paper examines the factors determining weld metal hydrogen cracking.

Fekken, *et al.* (Ref. 1), investigated hydrogen cracking in weld metals deposited using shielded metal arc, submerged arc and gas tungsten arc welding processes. The hydrogen content was varied by employing an Ar-5 vol-% H_2 shielding gas, and by exposing different electrode flux formulations in high-humidity high-temperature environments. Cracking was most prevalent in weld metals containing >3 ppm of diffusible hydrogen and more than 45% delta ferrite. Countermeasures such as soaking the weldment for 200 h at 200°C (392°F) after welding alleviated cracking. Although Fekken's study was comprehensive in scope, interactive parameters were varied during testing, *i.e.*, the electrode coating oxygen potential and weld metal chemistry changed when different proprietary SMA consumables were used. The delta ferrite content was varied by buttering and by altering the dilution during welding. The welding speed was decreased so that the cooling rate after welding was changed, and so on. The extensive scope of the test matrix possibly accounted for the scatter found in Fekken's test results. Also, the method of assessing hydrogen cracking susceptibility depended on three-point bend testing, and the use of bend test results for assessing the cracking susceptibility in actual welding situations is not straightforward.

Ogawa, *et al.* (Ref. 2), also examined hydrogen cracking in autogenous gas tungsten arc and plasma arc weld metals. In this study, weld metal chemistry was varied by altering plate chemistry. The hydrogen cracking susceptibility increased as the hydrogen content in the shielding gas increased (from 2 to 10% by volume) for weld metals containing >50% delta ferrite. Cracking initiated at the root of the weld and propagated in a transgranular manner through delta ferrite. The beneficial role of higher austenite levels in duplex stainless steel weld metal (in terms of decreasing hydrogen cracking susceptibility) was associated with a lower diffusible hydrogen content in test welds. Ogawa found that increasing weld metal nitrogen content from 0.05 to 0.15% increased the austenite content in weld deposits and markedly decreased hydrogen cracking susceptibility. In these tests, increasing deposit

KEY WORDS

Duplex Stainless
Stainless Steel Weld
Cold Cracking
Hydrogen Cracking
Crack Growth
Austenite Inhibitor
Crack Initiation Site
Cr_2N Precipitate
Nitrogen Effects
SERT Test/H_2 Cracking

K. SHINOZAKI is with the Department of Welding Engineering, Osaka University, Osaka, Japan. L. KE is a Research Engineer, Nanchang Institute of Aeronautical Technology, Nanchang, China. T. H. NORTH is WIC/NSERC Professor, Department of Metallurgy and Materials Science, University of Toronto, Canada.

Table 1 — Base Metal and Electrode Chemistries (wt-%)

		C	Mn	Si	Cr	Ni	Mo	N[(a)]	NiEq	CrEq
Base Metal		0.022	1.47	0.42	21.9	5.5	3.05	1370	6.90	25.58
	FM-1	0.022	1.1	0.36	22.0	4.0	3.0	1100	5.21	25.54
	FM-2	0.03	1.5	0.5	22.0	5.5	3.0	1500	7.15	25.75
Electrodes	FM-3	0.029	1.45	0.48	22.0	8.0	3.0	1400	9.60	25.72
	FM-4	0.029	1.40	0.47	22.0	10.0	3.0	1400	11.54	25.71
	FM-5	0.026	1.31	0.44	22.0	14.0	3.0	1300	15.44	25.11

(a) Nitrogen is in ppm.

Table 2 — Weld Metal Analysis

	C	Mn	Si	Cr	Ni	Mo	N	Ni(e)
W-1	0.022	1.28	0.38	21.99	4.90	2.86	0.081	6.20
W-2	0.030	1.53	0.45	22.06	5.71	2.81	—	7.38
W-3	0.029	1.47	0.49	21.98	7.57	2.84	—	9.18
W-4	0.028	1.52	0.45	22.09	9.00	2.78	—	10.60
W-5	0.022	1.45	0.43	22.10	12.36	2.82	—	13.75

nitrogen content produced the same effect as increasing the nickel equivalent of the steel chemistry, *i.e.*, it was nitrogen's role as an austenite stabilizer which was associated with decreasing cracking susceptibility. However, increasing weld metal nitrogen content also increases the driving force for chromium nitride precipitation in delta ferrite, and consequently, it is important to consider the dual effects of nitrogen on the austenite/ferrite balance and on chromium nitride precipitation.

The ferrite/austenite transformation depends on a number of factors, *i.e.*, on weld metal composition, cooling rate and time at temperature. The partition of Cr, Ni, Mo and N between austenite and ferrite has been examined by Ogawa and Kosecki (Ref. 3), and by Liljas, *et al.* (Ref. 4). In weld metal, there is limited partition of nickel, chromium and molybdenum between ferrite and austenite. However, nitrogen does partition and high nitrogen levels (around 0.3 to 0.4%) have been detected in the austenite phase (Ref. 4). This partitioning of nitrogen between austenite and ferrite leads to the formation of denuded (precipitate-free) grain boundary regions in weld metal. Svensson and Gretoft (Ref. 5) have indicated that the ferrite/austenite transformation temperature is increased when the nitrogen content of the weld is raised, and that a change in nitrogen content has a significant effect on the resulting weld metal microstructure. Deposits containing 973 ppm nitrogen had more Widmanstätten austenite compared to lower nitrogen content welds, and weld metal containing 630 ppm nitrogen had a microstructure where the austenite was mainly precipitated within the ferrite grains. The austenite/ferrite morphology has a large influence on nitride precipitation since precipitate formation is limited when the austenite nodules are in close proximity (Ref. 6). High cooling rates after welding limit the ferrite/austenite transformation and decrease the content of austenite in solidified weld metal. However, the presence of very high cooling rates will not prevent nitride precipitation. In this connection, Hertzman, *et al.* (Ref. 6), has indicated that nitride precipitation cannot be prevented even when the cooling rate is as great as 2500°C/s (4600°F/s).

Liljas, *et al.* (Ref. 4), has shown that gas tungsten arc and plasma arc welds produced at a heat input of 0.5 to 0.7 kJ/mm (12.7–17.8 kJ/in.) in high-nitrogen-content steel may contain around 60 to 65% ferrite. At lower heat input levels (around 0.1 kJ/mm; 2.5 kJ/in.,) his welds contained as high as 90% ferrite.

Assuming that delta ferrite is the phase that is crack sensitive (Ref. 2), the presence of extensive nitride precipitation in duplex stainless steel welds containing around 60% ferrite may have an important effect on hydrogen cracking susceptibility.

The Trap theory of hydrogen embrittlement suggests that precipitates and oxide inclusions will act as irreversible hydrogen traps and that their location and morphology can markedly affect hydrogen cracking susceptibility (Refs. 7, 8). A fine distribution of spheroidal second-phase particles will decrease cracking susceptibility since they will decrease the likelihood of exceeding the critical hydrogen content required for crack nucleation. However, the presence of needle-like precipitates, and in particular, when these precipitates are located at points of weakness (such as grain boundaries) will have a detrimental influence on cracking resistance (Refs. 8, 9). In a similar manner, the type of precipitates, their morphology and location may have a marked influence on the cracking susceptibility of duplex stainless steel weld metal. Cleavage of the ferrite matrix occurs preferentially along the cube planes (the {100} planes), and if chromium nitride precipitates are preferentially located on these planes, they may be extremely detrimental in terms of hydrogen cracking susceptibility.

This paper examines the effect of changing the ferrite/austenite balance on the susceptibility of duplex stainless steel weld metal to hydrogen cracking, and, in particular, the influence of nitrogen on the cracking susceptibility. The likelihood of cracking is evaluated using laboratory weldability tests, *i.e.*, using longitudinal-butt tensile restraint cracking (LB-TRC) (Ref. 10) and the weld metal slow extension rate (WMSERT) cracking tests. These weldability tests are particularly effective when monitoring changes in cracking susceptibility, in fractography of broken test samples, and in the microstructure of different weld samples. In this work, the weld metal chemistry was varied by al-

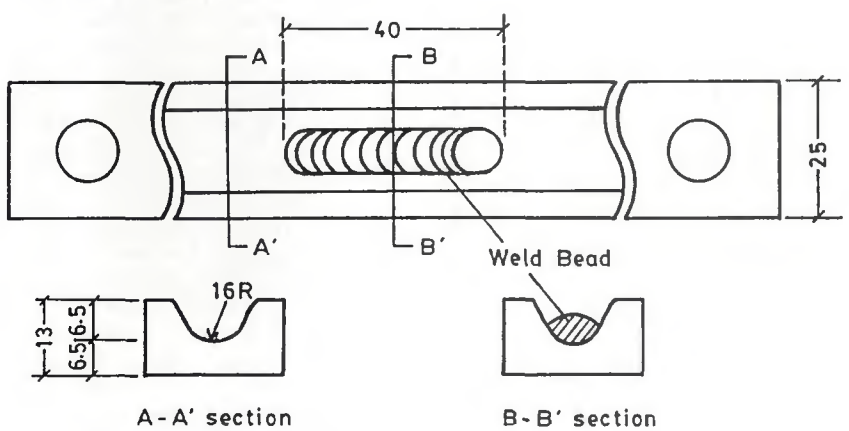

Fig. 1 — LB-TRC test configuration. B–B' indicates the slit prior to testing.

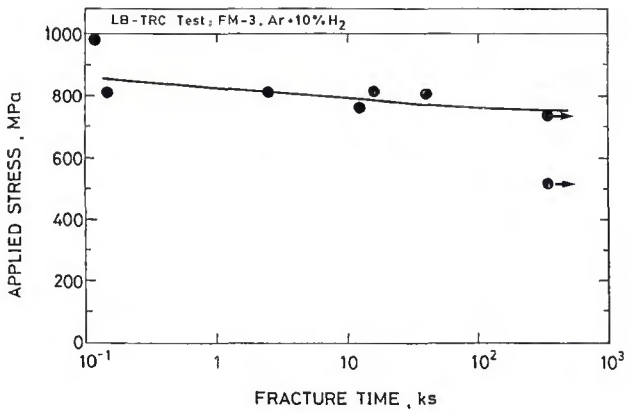

Fig. 2 — Relation between the applied stress and the time to fracture during LB-TRC testing. Weld metal W-3 containing 70% ferrite.

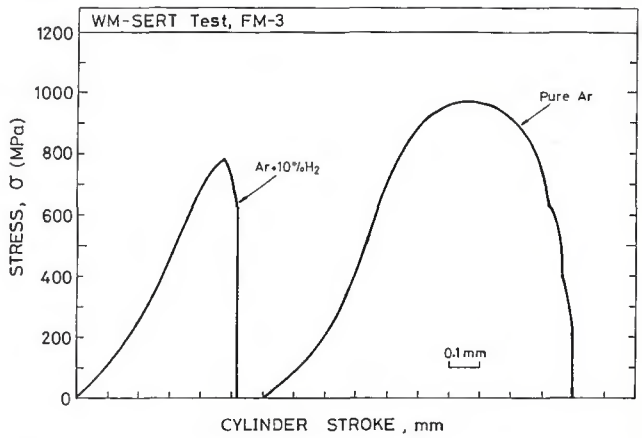

Fig. 4 — Applied stress/cylinder stroke relations during WM-SERT testing when using Ar and Ar-H_2 shielding gases. Weld metal W-3 containing 70% ferrite.

tering the electrode chemistry during gas tungsten arc welding with a shielding gas comprising Ar-10 vol-% H_2. In tests examining the effect of nitrogen in cracking susceptibility, the nitrogen content was varied using a specially formulated electrode composition/buttering procedure.

Experimental Procedure Materials

The base material used was 2205 duplex stainless steel with a nominal composition of 22 wt-% Cr 5 wt-% Ni 3 wt-% Mo. Five different laboratory-made filler metal wires were formulated, which produced varying ferrite contents during gas tungsten arc welding. Table 1 shows the base material and filler metal compositions. The weld metal analyses are presented in Table 2.

Longitudinal Butt-Tensile Restraint Testing

The LB-TRC test was developed by one of the authors to evaluate the cold cracking susceptibility of high-strength steel weld metals (Ref. 10). In this test, two plates are buried together providing a slit across which the weld bead is deposited — Fig. 1. A constant tensile load is applied in a direction parallel to the weld line when the weld temperature cools to 150°C (302°F) and the time to failure is evaluated. The critical stress level (σ_{CR}) above which weld metal cracking occurs in a 96-h period is the qualitative estimate of hydrogen-induced cracking susceptibility. All welds were produced using gas tungsten arc welding using Ar and Ar-10 vol-% H_2 shielding gas mixtures. The welding conditions were 200 A, 15 V and a welding speed of 1.67 X 10^{-3} m/s. The applied stress during testing was evaluated by dividing the applied load by the cross-sectional area of broken test samples.

Weld Metal Slow Extension Rate Tensile Testing

Constant loading tests such as LB-TRC testing have been widely used for evaluating hydrogen-induced cracking susceptibility in low-alloy steel weld metals. However, when this form of test is employed in duplex stainless steel weld metals, the duration of testing is necessarily prolonged since the diffusivity of hydrogen is low in austenite (Ref. 1). It is well known that hydrogen embrittlement is affected by strain rate, and consequently, slow extension rate tensile tests have generally been used to evaluate the effect of hydrogen on base metal mechanical properties (Refs. 11, 12), and on HAZ cracking susceptibility (Ref. 13). The test specimen design and welding parameters employed during WM-SERT testing were those in LB-TRC testing. All testing was carried out ten minutes after welding using a MTS servo-hydraulic tensile machine operating in the stroke-controlled mode. A constant stroke rate of 10^{-7} m/s was employed when assessing the cracking susceptibility of welds deposited using Ar-10 vol-% H_2 shielding gas mixtures. Some experiments were also carried out using higher stroke rates (3.13 X 10^{-7} m/s and 10^{-6} m/s) to evaluate the effect of this variable on test results. The initial section length of test specimens was 440 mm (17 in.). After deposition and testing of 40-mm (1.6-in.) long weld beads, the welded region was cut off and testing was repeated until the section length was 170 mm (6.7 in.). At this point, the remaining unused section length was discarded. The effect of section length changes on the extension rate during tensile testing was negligible (Appendix 1). The WM-SERT test results for hydrogen-free weld metal were evaluated by depositing weld beads using argon shielding gas, setting them aside for 24 hours and then tensile testing at a stroke rate of 10^{-5} m/s.

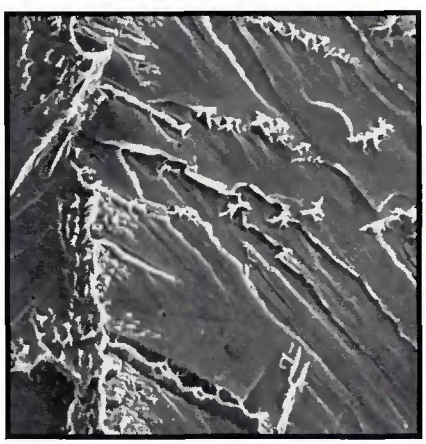

Fig. 3 — Fracture surface of an LB-TRC test specimen. Weld metal W-3 containing 70% ferrite.

Nitrogen Content Variation

It has been discussed previously that increasing nitrogen content increases the austenite content of stainless steel weld metal, changes the morphology of the ferrite and austenite phases, and promotes chromium nitride precipitation. It follows that nitrogen's role in terms of hydrogen cracking must be assessed using a test matrix, which specifically avoids confounding the test results, *i.e.*, the testing setup must separate nitrogen's precipitate formation capability from its austenite promotion capability.

In this study, the effect of nitrogen variation on the cracking susceptibility of fully ferritic weld metal was examined. A special buttering procedure was developed to evaluate the influence of weld metal nitrogen content on the hydrogen cracking susceptibility, namely: 1) Grooved WM-SERT specimens were

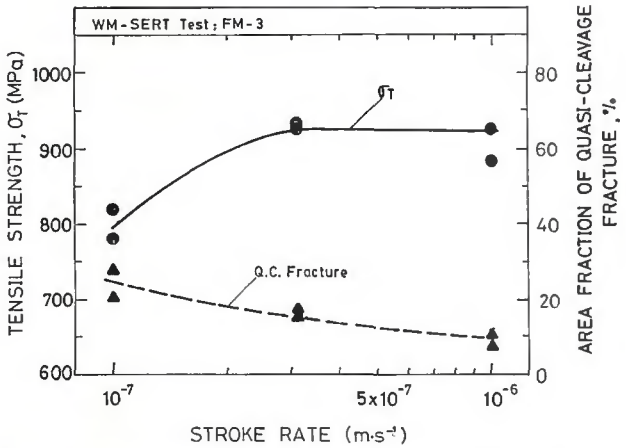

Fig. 5 — Effect of stroke rate on the peak tensile stress during WM-SERT testing (σT), and on the area fraction of quasi-cleavage failure. Weld metal W-3 containing 70% ferrite.

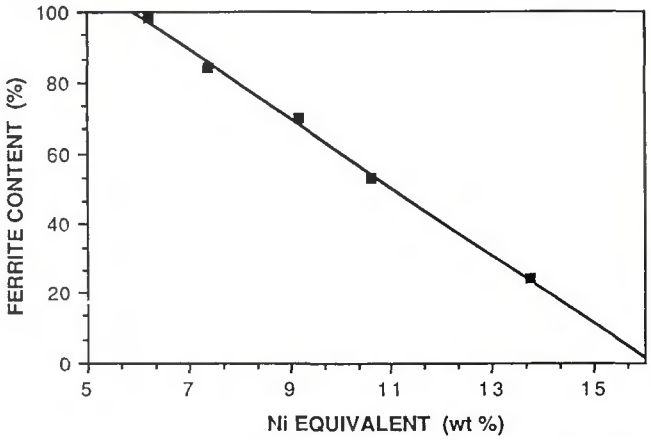

Fig. 6 — Relation between nickel equivalent and ferrite content measured using point counting.

buttered using electrodes of the first composition listed in Table 1. The welding parameters employed were those indicated previously, and the specimens were remachined to leave a low-nitrogen content layer in the base of the groove. 2) The test welds were then deposited using the electrode compositions identified as A and B in Table 1, and WM-SERT testing was carried out using the procedures indicated previously.

The weld metal diffusible hydrogen content in fully ferritic weld metal was measured using the International Institute of Welding (IIW) mercury method. There was no effect of nitrogen content variation (from 185 to 436 ppm) on deposit hydrogen content, and the deposit diffusible hydrogen content was 7 ppm when welding using Ar-10% H_2 shielding gas.

Delta Ferrite Measurement

A range of methods for delta ferrite measurement is available (point counting, ferrite scope and magne gauge testing). In this study delta ferrite content was measured using point counting and magne gauge testing. During point counting, twenty fields containing 81 points were examined at 500X magnification in samples FM-1, 2, 3 and 4. In sample FM-5 40 fields were examined. During magne gage testing, the weld cross-sections were ground smooth using No. 600 grit emery paper and magne gauge readings were taken according to the extended Ferrite Number (FN) method developed by Kotecki (Ref. 14). The highest values among six magne gauge readings on four different weld areas were averaged for any specimen.

Metallography

The test specimens were etched electrochemically in 10% oxalic acid and ethanol 10% hydrochloric acid solutions. The precipitate density in delta

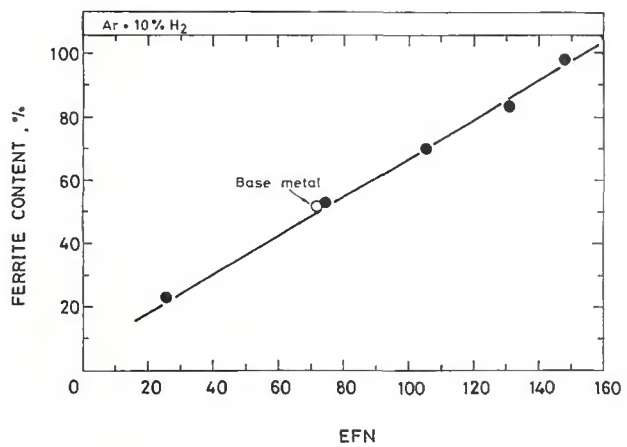

Fig. 7 — Relation between the extended ferrite number (FN) and the ferrite content found using point counting.

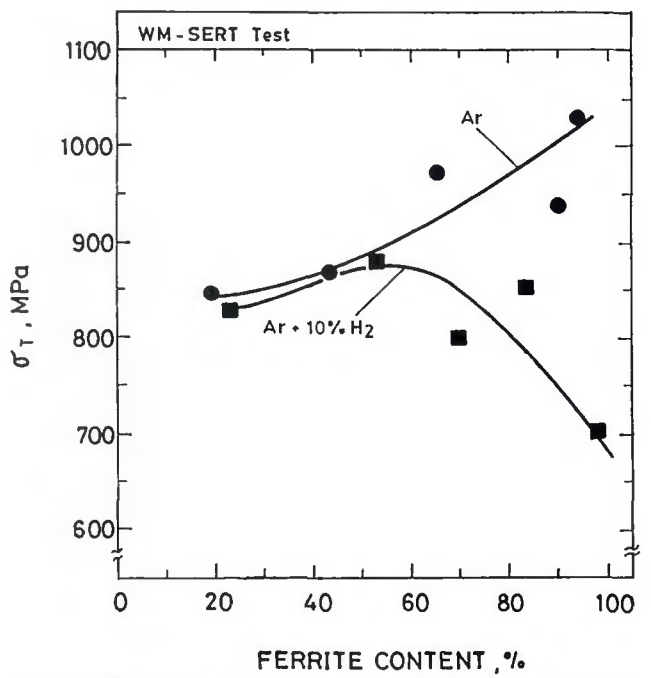

Fig. 8 — Effect of ferrite content on σT values when using Ar and Ar-H_2 shielding gases.

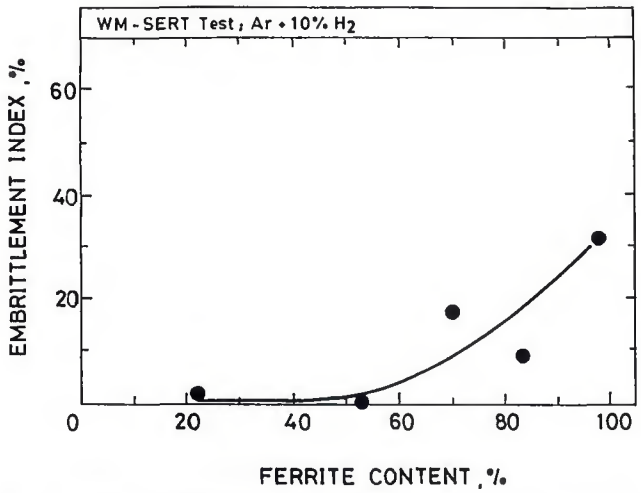

Fig. 9 — Effect of ferrite content on the hydrogen cracking susceptibility of duplex stainless steel weld metal. The embrittlement index is given as (NTS-LCS/NTS), where the NTS and LCS values are the test results produced using Ar and Ar-H_2 shielding gases.

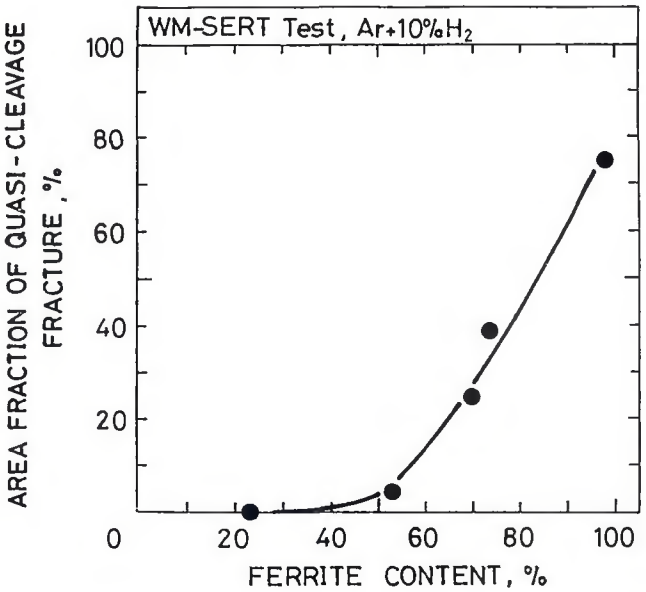

Fig. 10 — Relation between the area fraction of quasi-cleavage fracture on WM-SERT test specimens and ferrite content in duplex stainless steel weld metal.

ferrite was evaluated by counting particles in 50 fields using a magnification of 10,000X in an SEM microscope. The area fraction of quasi-cleavage failure on LB-TRC and on WM-SERT specimen fracture surfaces was measured by point counting using SEM photographs taken at 20X magnification.

Results

Figure 2 shows the applied stress/fracture time relation for weld metal containing 70% delta ferrite (Sample FM-3). The time to failure increased with decrease in the applied stress, and at stress levels less than 800 MPa (116 ksi), the test specimens were uncracked when the load was maintained for a period of 96 h. Figure 3 shows the typical fracture surface produced during LB-TRC testing, *i.e.*, comprising quasi-cleavage fracture with river pattern markings and numerous tear ridges. It is apparent from Fig. 2 that the LB-TRC test has limitations when estimating the weldability of duplex stainless steel weld metal, namely, a large number of test specimens are needed to establish the σ_{CR} value, the 96-h test requirement for each specimen makes the testing cycle prolonged, and the scatter in output results accentuates the above problems — Fig. 2. Because of these problems, the weld metal slow extension rate (WM-SERT) testing was examined as an alternative approach.

Figure 4 shows applied stress/stroke rate relations for duplex stainless steel weld metal containing 70% delta ferrite (FM-3), deposited using argon and Ar-10 vol-% H_2 shielding gases. The marked difference in the results when using argon and argon/hydrogen shielding gases suggested that the peak tensile strength value (σT) during WM-SERT testing might be a useful index of hydrogen cracking susceptibility. The validity of this assumption was confirmed by comparing (σT) results and LB-TRC (σ_{CR}) values. Figure 5 shows the relation between stroke rate and σT values. At the lowest stroke rate (10^{-7} m/s) the σT value decreased to around 800 MPa (116 ksi), and the area fraction of quasi-cleavage fracture on broken WM-SERT test specimens was highest — Fig. 5. The σT value produced during WM-SERT testing at a stroke rate of 10^{-7} m/s was similar to the critical stress level (σ_{CR}) found during LB-TRC testing of weld metal of equivalent composition (compare Figs. 2 and 5). Moreover, the area fraction of quasi-cleavage fracture on WM-SERT samples was similar to that found during LB-TRC testing. Since the LB-TRC test has proved to be an extremely effective monitor of hydrogen cracking susceptibility in high-strength steel weld metals (Ref. 10), the close correlation between σT and σ_{CR} values in this study validates the use of σT values as a measure of duplex stainless steel weld metal weldability.

Figure 6 shows the relation between delta ferrite content and nickel equivalent values (based on point counting results). It is clear that the ferrite content in the base metal is much less than that in weld metal having the same nickel equivalent value. This occurs since the base metal ferrite content is critically dependent on factors such as prior heat treatment and thermal cycle. Figure 7 shows the relation between the extended ferrite number (FN) and deposit ferrite content found by point counting. The regression relation is,

$$\text{ferrite content} = 0.6\,(\text{FN}) + 6 \qquad (1)$$

This relationship is very similar to that indicated by Liljas, *et al.* (Ref. 4), namely,

$$\text{ferrite content} = 0.59\,(\text{FN}) + 4.5 \qquad (2)$$

Because of the clear-cut relation between ferrite content and FN number, magne gauge testing was employed as the principal tool when evaluating the delta ferrite content of weld samples.

Figure 8 relates WM-SERT cracking susceptibility (σT values) with weld metal ferrite content (for weld metals deposited using argon and Ar-10 vol-% H_2 shielding gases). In welds deposited using argon shielding gas, σT values increased as ferrite content increased. On

Table 3 — Effect of Nitrogen Content on s_T Values in 100% Ferrite Weld Metal

Shielding Gas	Nitrogen (ppm)	σ_T (MPa)	Hardness (VPN)
Argon	190	564.4	235
Ar-10%H_2	213	234.0	254
NTS-LCS/NTS = 0.59			
Argon	467	827.2	254
Ar-10%H_2	469	292.6	259
NTS-LCS/NTS = 0.65			

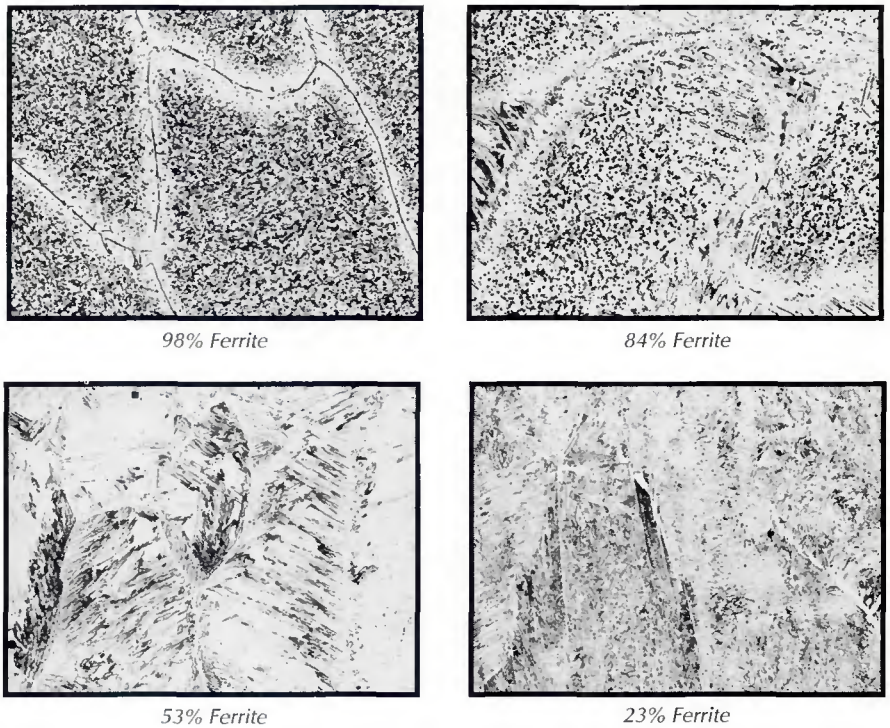

Fig. 11 — Weld metal microstructures containing a range of ferrite contents. Magnification 350X.

the other hand, they decreased when the delta ferrite content exceeded 50% in welds deposited using Ar-10 vol-% H_2 shielding gas. It follows that duplex stainless steel weld metals containing more than 50% delta ferrite are susceptible to hydrogen cracking. The hydrogen embrittlement index (NTS-LCS/NTS), where NTS is the notched tensile strength and LCS is the lower critical stress, has been commonly used as a measure of hydrogen cracking susceptibility (Refs. 15, 16). If the σT values produced in Ar and Ar-10 vol-% H_2 weld deposits are taken as the NTS and LCS values, the hydrogen embrittlement index increases markedly when the delta ferrite content exceeds 50% — Fig. 9.

Table 3 shows replicated test results illustrating the effect of weld metal nitrogen content on σT and hardness values. During gas tungsten arc welding with pure argon shielding gas, an increase in weld metal nitrogen content markedly increased the σT value and only had a small effect on weld metal hardness. When Ar-10% H_2 shielding gas was used a similar change in nitrogen content increased σT but had little influence on weld zone hardness values. The effect of increasing nitrogen content on the embrittlement index (NTS-LCS/NTS) was evaluated. Taking the NTS and LCS values as the σT results when welding using pure argon and Ar-10% H_2 shielding gases, the embrittlement index increased from 0.59 to 0.65 when the weld metal nitrogen content was increased. These results indicate that increasing weld metal nitrogen content increases the hydrogen cracking susceptibility of the ferrite phase.

Discussion

Hydrogen induced cracking in duplex stainless steel weld metal markedly depends on the delta ferrite content. Ogawa, *et al.* (Ref. 2), has suggested that since the hydrogen has an extremely low diffusivity in the austenite phase, any decrease in delta ferrite content (as the nickel equivalent is increased) decreases the diffusible hydrogen content available for crack initiation. The area fraction of quasi-cleavage failure on weld specimens produced using Ar-10 vol-% H_2 shielding gas increased as the delta ferrite content increased — Fig. 10, and this relationship closely parallels that between cracking susceptibility and delta ferrite content.

Beachem's model for hydrogen cracking indicates that hydrogen promotes crack extension by favoring dislocation movement and that the fracture surface morphology on broken test specimens depends on the critical hydrogen content at the crack tip region and the stress intensity level applied (Ref. 17).

For the same hydrogen content in the steel, increasing stress intensity changes the mode of fracture from intergranular to quasi-cleavage, and then to microvoid coalescence. Also, for any testing situation, increasing the diffusible hydrogen content will promote the formation of intergranular, quasi-cleavage or microvoid coalescence failure modes at lower stress intensity levels.

Since Ar-10 vol-% H_2 shielding gas was used throughout during WM-SERT testing, the hydrogen content absorbed by the weld metal was unchanged during testing. However, the available diffusible hydrogen content will vary when the ferrite content changes (since austenite has higher solubility for hydrogen, and since the diffusion rate of hydrogen in austenite at room temperature is extremely low). It follows that the presence of greater amounts of quasi-cleavage fracture on broken WM-SERT test specimens is indicative of increased hydrogen being available at the crack tip region and consequently these results support Ogawa's contention that decreased ferrite content produces lower diffusible hydrogen contents (Ref. 2).

However, since the duplex weld metal microstructure comprises crack susceptible ferrite and tough austenite, the ferrite/austenite morphology in weld metal will have a strong influence on hydrogen crack propagation.

Figure 11 shows the weld metal microstructures containing varying delta ferrite contents (98 to 23%). Widmanstätten austenite plates are clearly apparent in deposits containing 98 and 84% delta ferrite — Fig. 11A and B. Intergranular austenite plates occur in welds containing 70 and 53 % ferrite — Fig. 11C and D. The etch pits associated with extensive precipitation in delta ferrite are clearly apparent in Fig. 11A, B and C. Only the regions adjacent to the

98% Ferrite

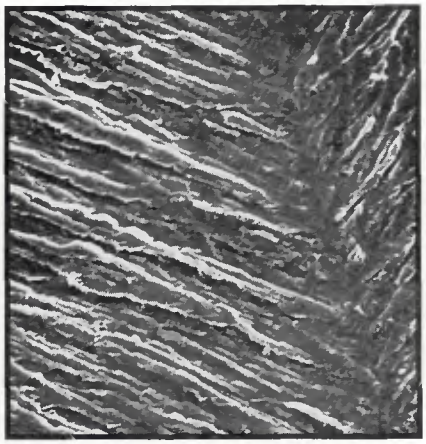

84% Ferrite

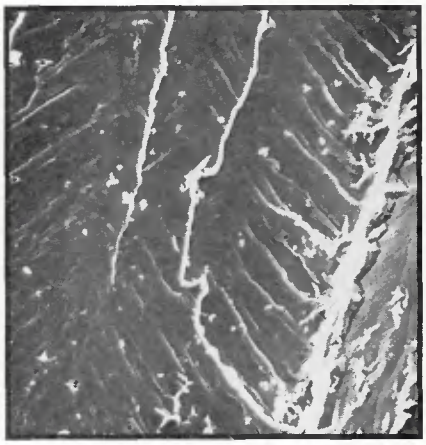

70% Ferrite

53% Ferrite

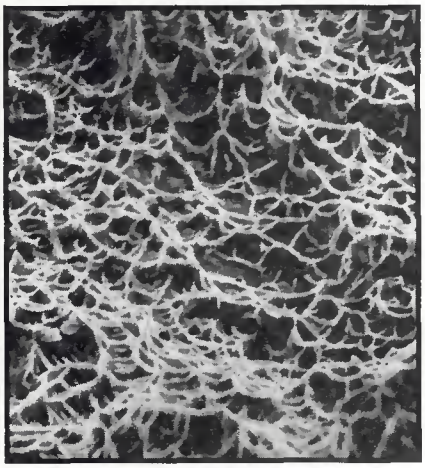

23% Ferrite

Fig. 12 — Fracture surface morphologies of weld metals containing a range of delta ferrite contents. Ar-10% H_2 shielding gas used throughout. Magnification 1200X.

grain boundaries were free of extensive precipitation — Fig. 11A.

Figure 12 shows the fracture surface morphologies in samples containing different ferrite contents (98, 84, 70, 53 and 23%, respectively). In weld metal containing 98% ferrite, the fracture surface was macroscopically flat, with numerous parallel facets. This fracture surface morphology is quite different from conventional cleavage fracture and, for the purposes of this paper, it is termed quasi-cleavage failure. When the ferrite content decreased, tear ridges and slip lines were formed on specimen fracture surface — Fig. 12D. Microvoid coalescence failure was only observed in specimens containing 23% ferrite — Fig. 12E. Based on the diverse microstructures shown in Fig. 11 and the fracture surface morphologies in Fig. 12, a model is tentatively suggested which relates hydrogen cracking susceptibility with weld metal microstructural changes.

Both Perng (Ref. 11) and Ventakatasubramanian (Ref. 18) observed that the austenite phase in duplex stainless steel base material suppresses slow crack growth during hydrogen embrittlement. Assuming that crack propagation during hydrogen cracking will depend on attainment of a certain critical stress just ahead of the crack tip, the value of this fracture stress depends on the composition and microstructure of the steel, and on the local hydrogen concentration.

The presence of austenite in the duplex microstructure has two important effects: 1) it reduces the hydrogen concentration ahead of the crack tip (because of its influence on hydrogen permeability); and 2) bridging of the propagating crack by austenite will increase the local stress required for the fracture process.

It is clear from Fig. 11 that as the delta ferrite content decreases austenite plates grow into the ferrite matrix, and transgranular austenite is formed in welds containing 70 and 53% ferrite.

Based on these observations, it is suggested that crack growth in duplex weld metal is likewise suppressed by austenite plates. The increased frequency of tear ridges on the fracture surfaces in welds containing decreasing ferrite content supports this contention. Also Fig. 13 confirms that the tear ridges formed

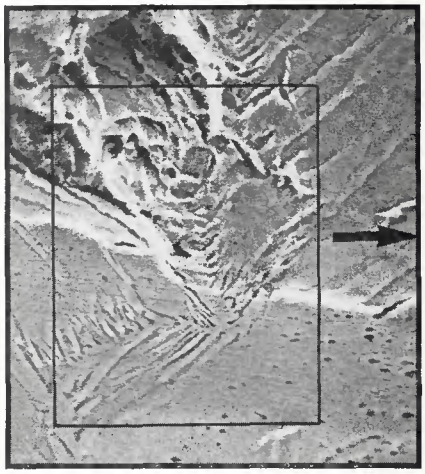

Fig. 13 — Correspondence between the ductile tear region on the fracture surface of a broken WM-SERT test specimen and the austenite plates in the weld metal microstructure. Specimen W-3 containing 70% ferrite. Magnification 1467X.

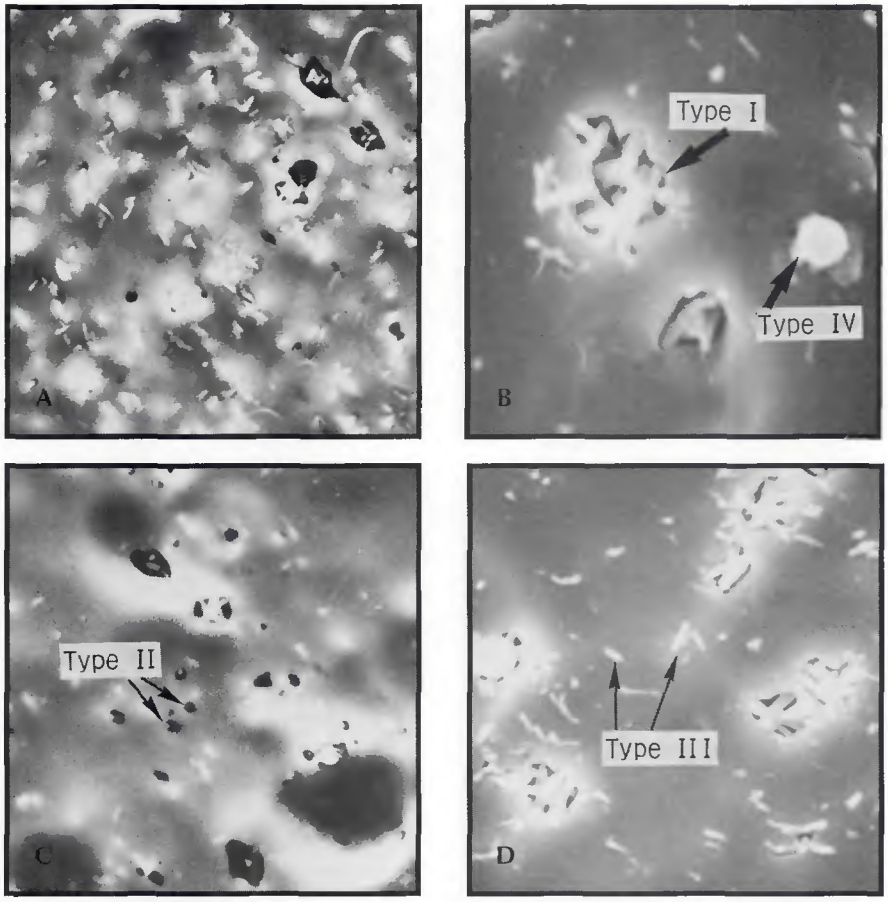

Fig. 14 — Modes of precipitation in weld metal containing 98% ferrite. A — General view (5000X); B —Type I and Type IV precipitates (13750X); C — Type II precipitates (6880X); D — Type III precipitates (9167X).

on the fracture surface of a specimen containing 70% ferrite are produced when austenite plates are ruptured. In this connection, Kamiya, *et al.* (Ref. 19), has examined the toughness of duplex stainless steel weld metals containing different ferrite/austenite ratios. The ferrite/austenite transformation follows the Kurdjamov-Sachs's relationship where the (111) plane in austenite and the (110) plane in ferrite are parallel, and this creates a coherent interface which resists fracture. When the austenite plates are large enough, the austenite phase fails by microvoid coalescence.

Figure 14 shows the modes of precipitation in weld metal containing 98% ferrite. Four distinct morphologies were apparent — Figs. 14A–D: Type I — angular-shaped Cr_2N-oxide particle combinations; Type II — acicular-shaped Cr_2N precipitates; Type III —cluster-shaped Cr_2N precipitates; Type IV — spherical oxide inclusions

In this connection, Hertzman, *et al.* (Ref. 6), has calculated that CrN is more stable than CrN in the temperature range 750° to 1100°C (1382°–2012°F) in duplex stainless steel microstructures. The amount of Type I, II and III precipitation increased when the weld metal ferrite content increased — Fig. 15. As would be expected, the content of oxide inclusions (Type IV particles) was unaffected by change in weld metal ferrite content. The results in Table 3 indicate that increasing nitrogen content in fully ferritic weld metal increases the susceptibility to hydrogen embrittlement.

It has already been shown that Cr_2N precipitation promotes brittle fracture in duplex stainless steel (Ref. 5) and in high-purity 30% Cr-2% Mo steel (Ref. 20). Also, precipitation of chromium and titanium carbides in body-center-cubic materials (Ref. 7), and graphite in nickel (Ref. 9) produce sites for hydrogen entrapment and crack initiation. Kokawa, *et al.* (Ref. 21), has examined Cr_2N precipitation in duplex and fully ferritic stainless steel weld metals and confirmed the following effects:

1) The facets on the fracture surfaces of broken WM-SERT test specimens in weld metal containing 98% ferrite (weld metal W1 in this study) are parallel to the cleavage plane in delta ferrite, the (100) plane in the bcc lattice.

2) The growth direction of Cr_2N precipitates in ferrite is the [100] direction and the nitrides are parallel to the {100} planes in ferrite. Also, the long axis of the needle-like Cr_2N precipitates ismore coherent with the ferrite matrix than the tips of the precipitates. It follows that the tips of Cr_2N precipitates may act as irreversible sinks for hydrogen, and may act as crack initiating sites.

3) Cr_2N precipitates are nucleated at solidification sub-boundaries and at oxide inclusions in the weld metal — Fig. 16.

It is therefore suggested that the presence of chromium nitride precipitation in ferrite will make this product more sensitive to hydrogen cracking. These results appear to contradict Ogawa's results, which indicate that increasing nitrogen content in duplex stainless steel weld metal decreases hydrogen cracking susceptibility (Ref. 2). However, Ogawa's results depended on nitrogen increasing the content of austenite in duplex stainless steel weld deposits. In effect, it was nitrogen's role as an austenite stabilizer that produced the beneficial effect of higher nitrogen content. It follows that if nitrogen is added to argon shielding gas, and this produces more austenite in the weld deposit, this will be beneficial in terms of hydrogen cracking resistance. However, if high nitrogen content duplex stainless steel weld metal is deposited so that it contains > 50% ferrite there will be significant amounts of Cr_2N precipitation in the ferrite phase. Liljas, *et al.* (Ref. 4), has already indicated that deposits produced at a heat input of 0.5 to 0.7 kJ/mm in high nitrogen content plate contained > 60% ferrite, and lower heat input levels raised the ferrite level to as high as 90%. In this case, the presence of nitride precipitation may produce sites for hydrogen crack initiation in ferrite.

Also, the possible interaction of nitride precipitation with weld metal oxide inclusions may have important implications. Duplex stainless steel weld metals produced using shielded metal arc, submerged arc and gas metal arc welding contain significant oxygen contents (in the range 250 to 850 ppm). One might speculate that changes in the oxide particle distribution and in inclusion chemistry (caused by variations in the oxygen potential of the flux formulation or shielding gas) and the concomitant nitride precipitation might have a synergic effect on the hydrogen cracking susceptibility of oxygen-bearing weld metal.

Conclusions

LB-TRC and WM-SERT testing were used to evaluate the hydrogen cracking susceptibility of duplex stainless steel weld metal. WM-SERT testing was em-

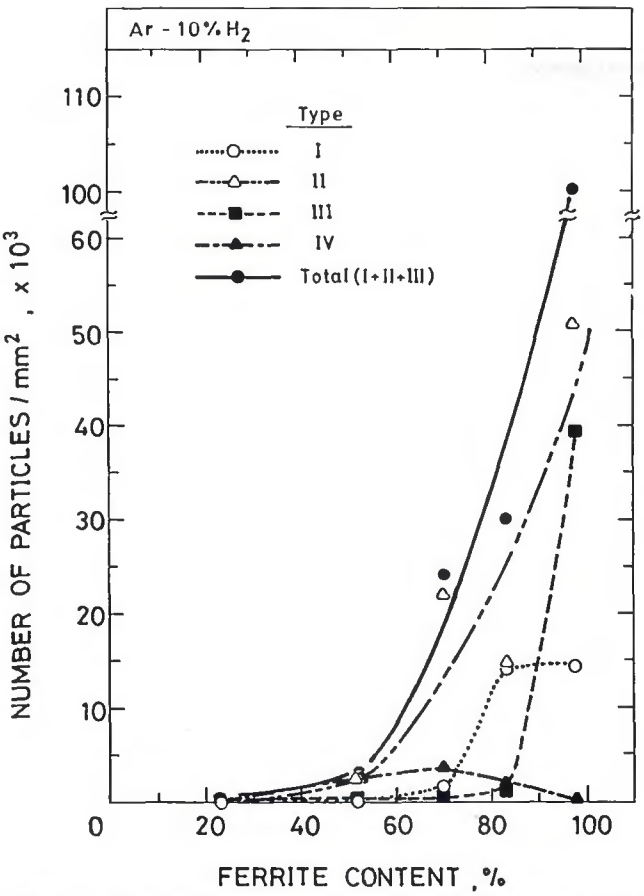

Fig. 15 — Relation between precipitation and ferrite content in the weld metal microstructure.

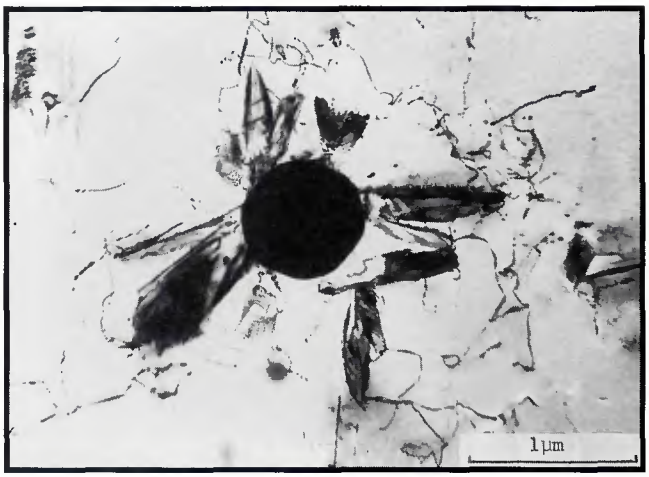

Fig. 16 — Cr_2N precipitates nucleated by oxide inclusions in the weld metal.

ployed for the examination of weld metal containing a range of delta ferrite contents. WM-SERT testing provided a qualitative estimate of hydrogen induced cracking susceptibility and allow detailed evaluation of the effects of deposit microstructure (austenite phase morphology) and of weld metal nitrogen content on cracking. The principal conclusions are as follows:

1) Hydrogen cracking occurs in duplex stainless steel weld metal containing 70% delta ferrite when test specimens are subjected to constant loading during LB-TRC testing. WM-SERT testing at a stroke rate of 10^{-7} m/s can be used in place of LB-TRC testing for monitoring hydrogen-induced cracking susceptibility. The monitor of cracking susceptibility in this case is the peak stress (σT) attained during testing.

2) The hydrogen cracking susceptibility increases markedly when the delta ferrite content increases above 50% in weld deposits produced using an Ar-10 vol-% H_2 shielding gas. Fractographic examination indicated that hydrogen crack growth in the duplex was inhibited by intergranular austenite plates at prior delta ferrite grain boundaries. This effect was due to the presence of a coherent interface between the ferrite and austenite phases.

3) Increasing nitrogen content from 190 to 469 ppm in fully ferritic stainless steel weld metal increased the hydrogen cracking susceptibility. It is suggested that this detrimental effect of nitrogen on the cracking sensitivity of ferrite may be associated with the presence of Cr_2N precipitation in delta ferrite.

Appendix

Effect of Specimen Length on Extension Rate during WM-SERT Testing

The effect of specimen length on the extension rate in the notched region can be assessed using Fig. A-1. Ignoring stress concentration and machine realization effects, the extension rate in the notched section can be given as:

$$\Delta 1 = \Delta 1o + 2\Delta 1_1 \qquad \text{(A-1)}$$

$$\Delta 1o = \Delta 1 - (2\ 1_1/EA_1)\ P \qquad \text{(A-2)}$$

$$d\ \Delta 1o/dt = \Delta 1/dt - (2\ 1_1/EA_1)\ (d\ P/Dt) \qquad \text{(A-3)}$$

where $\Delta 1o$ = elongation of the notched region, $\Delta 1_1$ = elongation at section length, $\Delta 1$ = total elongation of specimen, P = load, E = Young's modulus and A_1 = specimen cross-section.

The notched region extension rate is proportional to the speed of loading, and Table 1-A shows the loading speed values obtained when testing different section lengths. Figure A-2 compares the stroke rate during testing with the loading speed. It is clear that the differences in loading speed produced due to changes in section length are negligible compared to the effect of stroke rate variations.

Table A-1 — Loading Speed for Different Section Lengths during WM-SERT Testing

Specimen length (mm)	Loading speed (N/s)
170	3.6
220	3.3
270	3.5
320	3.5
370	3.0
420	3.2

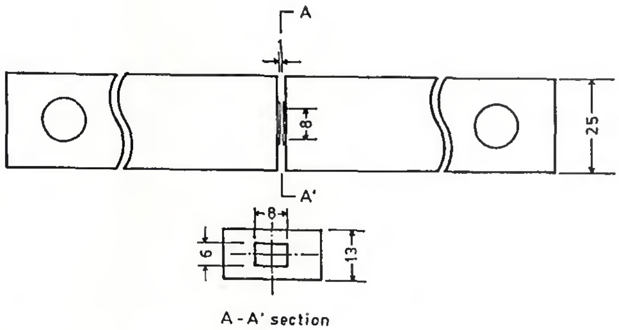

Fig. A-1 — The approximation used for analyzing weld zone dimensions during WM-SERT testing.

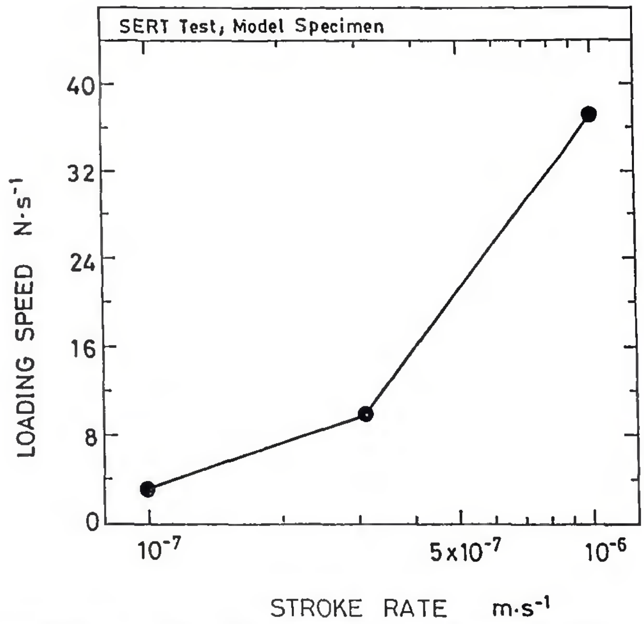

Fig. A-2 — Relation between loading speed and stroke rate during WM-SERT testing.

Acknowledgments

The authors wish to acknowledge the support provided by the Natural Science and Engineering Research Council of Canada and the Welding Institute of Canada.

References

1. Fekken, U., Nassau , L. van, and Verwey, M. 1986. Hydrogen induced cracking in austenitic/ferritic duplex stainless steel. *Proc. International Congress, Duplex Stainless Steel,* Netherlands, pp. 268–279.

2. Ogawa, K., Komizu, Y., and Miura, M. 1987. Investigation of the applicability of arc welding processes to duplex stainless steel offshore linepipe, IIW Doc., IIX-1461-87.

3. Ogawa, T., and Kosecki, T. 1988. Weldability of newly developed austenitic alloys for cryogenic service. *Welding Journal* 67:8-s to 17-s.

4. Liljas, M., and Qvarfort, R. 1986, Influence of nitrogen on weldments in UNS S 31803. *Proc. International Congress, Duplex Stainless Steel,* Netherlands, pp. 244–255.

5. Svensson, L. V., and Grethof, B. 1986. Property-microstructure relationships for duplex stainless steel weld metals. *Proc. International Congress, Duplex Stainless Steel.* Netherlands, pp. 288–294.

6. Hertzman, S., Roberts, W., and Lindenmo, M. 1986. Microstructure and properties of nitrogen alloyed duplex stainless steel after welding treatments. *Proc. International Congress, Duplex Stainless Steel,* Netherlands, pp. 257–267.

7. Pressouyre, G. M., and Bernstein, I. M. 1981. An example of the effect of hydrogen trapping on hydrogen embrittlement. *Metall. Trans. A,* 12A, pp. 835–844.

8. Pressouyre, G. M. and Zmudzinski, C. 1981. Influence of inclusions on hydrogen embrittlement. *Proc. Conf. Mechanical Working and Steel Processing,* XVIII, AIME, New York, N.Y.

9. Lee, T. S. F,. and Latinison, R. M. 1987. Effects of grain boundary segregation and precipitation on the hydrogen cracking susceptibility of nickel. *Metall. Trans. A,* 18A, pp. 1653–1662.

10. Matsuda, F., Nakagawa, H., and Shinozaki, K. 1979. The LB-TRC test for cold cracking susceptibility of weld metal for high-strength steels. *Trans. JWRI,* 8, p. 113.

11. Perng, T. P., and Altstetter, C. J. 1988. Cracking kinetics in two-phase stainless steel alloys in hydrogen gas. *Metall. Trans A,* 19A, pp. 145–152.

12. Costa, J. E., Williams, J. C., and Thompson, A. W. 1987. Effect of hydrogen on mechanical properties in Ti-10-2Fe-3Al. *Metall. Trans.,*18A, p. 1421.

13. Kitada, T., and Tanaka, J. Application of implant testing to weld cold cracking with particular reference to the influence of hydrogen. *Proc. Int. Cong., JIMS-2, Hydrogen in Metal,* Japan.

14. Kotecki, D. 1982. Extension of the WRC ferrite number system. *Welding Journal* 62: 352-s to 361-s.

15. Bonizewski, T., Watkinson, F., Baker, R. G. and Tremlett, H. F. 1965. Hydrogen embrittlement and heat-affected-zone cracking in low carbon alloy steels with acicular microstructures. *Brit. Weld. J.,* 12, p.14.

16. Sawhill, J. M., Dix, A. W., and Savage, W. F. 1974. Modified implant test for studying delayed cracking. *Welding Journal,* 53:554-s.

17. Beecham, C. D. 1972. A new model for hydrogen assisted cracking. *Metall. Trans.,* 3, p. 437.

18. Verkatasubramanian, T.V., and Baker, T. J. 1983. Enhanced stress corrosion resistance from steels having dual-phase austenite-martensite microstructures. *Metall. Trans.* A, 14A, p. 1921.

19. Kamiya, O., Kumagai, K., Kikuchi, Y., and Enjo, T. 1989. Effect of microstructure on fracture toughness of SUS329J1 duplex stainless steel welds. *Trans. Japan Weld. Soc.,* 20, pp. 76–83.

20. Ikawa, H., Nakao, Y., and Nishimoto, K. 1980. Embrittlement in the weld metal of high-purity 30 Cr-2 Mo steel. *Trans. Japan Weld. Soc.,* 11, p. 115.

21. Kokawa, H., Tsory, E., and North, T. H. Presented at the AWS Annual Meeting in Los Angeles, Calif.,1990.